Adhesion of moving droplets in microchannels

Haosheng Chen (陈皓生),[1] Enkai Dong (董恩凯),[2] Jiang Li (李疆),[2,a)] and Howard A. Stone[3,a)]
[1]*State Key Laboratory of Tribology, Tsinghua University, Beijing 100084, China*
[2]*School of Mechanical Engineering, University of Science and Technology Beijing, Beijing 100083, China*
[3]*Department of Mechanical and Aerospace Engineering, Princeton University, Princeton, New Jersey 08544, USA*

(Received 30 July 2013; accepted 10 September 2013; published online 23 September 2013)

When oil drops in a continuous water phase move from the hydrophilic to the hydrophobic section of a microchannel, they can be controlled to either adhere or not adhere on the channel by changing the capillary number. Using experiments and a model for the thin film flow, we show that the critical capillary number for adhesion is approximately $Ca \sim D^{3/4}/d^{3/2}$, where D and d is the length of the droplet and the inner dimension of the microchannel, respectively. As one application of these ideas, droplet adhesion is demonstrated as a promising technology for recycling of emulsions in droplet microfluidics. © *2013 AIP Publishing LLC*. [http://dx.doi.org/10.1063/1.4823456]

The adhesion of droplets to substrates is a common phenomenon in nature, such as water droplets adhering to the petals of a rose flower. Controlling adhesion has many applications in industry, such as self-cleaning glass, automobile paints, and tires on wet roadways.[1–4] In microfluidic systems, adhesion also happens when bubbles, droplets, and cells are transported in the microchannels,[5,6] and, in such cases, the wettability of the inner surfaces of the channels needs to be treated properly. In most circumstances, the inner surface of the channel is modified to be wetting for the continuous phase in order to prevent adhesion of suspended objects either in the flow-focusing or "T" junction geometries used for generation of emulsion droplets,[7–10] or in the lab-on-a-chip devices for cell assays.[11–13] Otherwise, the emulsion droplets may breakup, which can cause failure of the droplet flow. In other cases, the inner surfaces of the channels are designed to cause the adhesion of the droplets or cells so as to realize the separation of the cells from the continuous phase or to trigger drug release at specific targets. For example, nanostructured silicon substrates have been fabricated to achieve the selective adhesion of circulating tumor cells (CTC),[14] and in experiments on cell separation, different types of cells were demonstrated to have different adhesion behaviors on different functionalized surfaces.[15] Thus, the adhesion of moving droplets may influence the development of technologies for lab-on-a-chip applications.

The mechanism of droplet adhesion to a nearby substrate is due to the forces between the two approaching surfaces.[16] The adhesion force is usually measured with an atomic force microscope (AFM) operating on the different surfaces.[17,18] Recently, the adhesion of soft matter such as liquid droplets and bubbles has been studied,[19–21] and the interaction between the substrates was accompanied by deformation during the approach process. This adhesion problem will be more complex in the microfluidic applications mentioned above, because the droplet moves relative (tangential) to the channel surface, and the thickness of the lubricating film of the continuous phase that separates the droplets from the wall is affected by the translation speed. For example, Bretherton[22] predicted the thickness of a thin liquid film for a long bubble moving steadily in a homogeneous tube filled with liquid, and the theory was further generalized to an immiscible viscous drop[23,24] instead of an inviscid bubble. However, we are not aware of any study of the adhesion of droplets moving in microchannels.

Here, we study the adhesion of moving droplets in microfluidic systems by using a capillary device to generate oil droplets in a continuous water phase. The microchannel has two distinct sections in series, one hydrophobic and the other hydrophilic. We control droplet adhesion by adjusting the translation speed of the drops that enter the hydrophobic section. The critical capillary number, which is a dimensionless flow speed, to induce the adhesion of droplets was experimentally measured for different drop sizes and channel dimensions. In addition, we present a theoretical analysis based on (i) the Bretherton model of a bubble translating in a liquid-filled tube and (ii) a model of the surface force-induced instability of a thin film in order to derive the relation of the critical capillary number for adhesion to the geometric parameters. Finally, we provide a demonstration that this adhesion can be used as a promising technology for emulsion recycling in microfluidics.

Our experiments of droplet adhesion were performed in a microfluidic device, where oil-in-water emulsion droplets were generated and transported from an upstream hydrophilic section to a downstream hydrophobic section in a square capillary. The flow speeds of the continuous and dispersed phases were controlled by independent syringe pumps. A high-speed camera (Phantom Miro M110) with a 5× microscope objective lens was used to observe the adhesion at the hydrophilic-to-hydrophobic junction. The setup of the experiments is shown in Figure 1(a).

The microfluidic device consisted of a co-flowing structure for the generation of the droplets and a straight square capillary with modified wettability, as shown in Figure 1(b). A cylindrical glass capillary with an outer diameter of 1 mm was tapered by a pipette puller, and the tapered glass capillary was inserted into a square glass capillary to form the co-flow

a)Authors to whom correspondence should be addressed. Electronic addresses: lijiang@ustb.edu.cn and hastone@princeton.edu

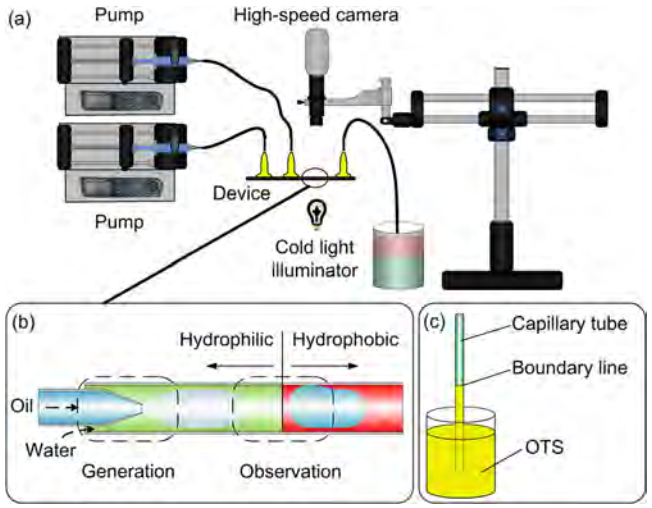

FIG. 1. Experimental setup. (a) Schematic of the droplet adhesion experiment. Two pumps were used to separately drive the inner and outer fluids in the capillary device to generate oil-in-water droplets; a high-speed camera was used to observe the adhesion of the droplets. (b) An enlarged sketch of the co-flowing structure of the capillary device with a hydrophobically treated glass channel. (c) Sketch of the approach to use the capillary wetting force to make half of the capillary hydrophobic. Typically, the hydrophilic part was 16 mm long and the hydrophobic part was 11 mm long.

structure, where oil-in-water droplets were generated. The continuous phase, which was an aqueous solution of 2 wt. % polyvinyl alcohol (PVA, Mw = 13000-23000 g/mol, 87%–89% hydrolyzed, Sigma-Aldrich), was injected into the interstices between the two capillaries, while the oil phase, which was liquid paraffin (Sinopharm Chemical Reagent Beijing Co.), was injected into the cylindrical capillary. PVA, which is a biocompatible and biodegradable material,[25] is often used as a surfactant in aqueous phases in many microfluidic applications. Both the flow rates of the aqueous and oil phases were controlled by syringe pumps, and the size of the oil droplets was changed by adjusting the flow rate ratio of the two phases. The surface tension between the two phases was $\gamma = 16.6$ mN/m, the viscosity of the aqueous phase was $\mu = 1.9$ mPa·s, and the viscosity of the oil phase was 28.9 mPa · s.

The straight square capillary with modified wettability was placed downstream of the co-flow structure. Three different square capillaries with inner dimensions of $d = 0.50$ mm, 1.05 mm, and 1.75 mm were treated chemically. The inner surface of the original square capillary was hydrophilic, and the downstream part of the square capillary was treated to be hydrophobic by immersing the capillary vertically into an octadecyltrichlorosilane (OTS) solution for 10 s before the device was made; a boundary line was marked on the outer surface of the square capillary according to the position of the OTS surface, as shown in Figure 1(c). Then, the capillary was rinsed with water from the untreated end. The mean squared value of the surface roughness of the OTS coated capillary was 15 ± 2.5 nm, as measured by an atomic force microscope (CSPM-4000). The contact angles of the hydrophilic section and the hydrophobic section were 11° and 90°, respectively. When the treated capillary was installed into the device, the upstream co-flow structure was formed within the untreated hydrophilic section, while the hydrophobic section was placed downstream.

Adhesion of the droplets on the hydrophobic surface was observed as the oil-in-water emulsion droplets were flowing past the hydrophobic part of the capillary, as shown in Figure 2(a). The oil droplets, which were dyed red (Sudan III, Sigma-Aldrich), adhered on the hydrophobic surface, and hence the oil-in-water emulsion was broken. The oil phase subsequently wetted the hydrophobic channel surface, and so encapsulated the water phase to form a water-in-oil emulsion. The process of the adhesion is illustrated by the time sequence of images in Figure 2(b).

Whether or not the oil droplets adhered to the hydrophobic surface depends on the speed and size of the droplets. For example, for a given drop size, faster droplets were observed to pass through the hydrophobic section without adhesion, while those moving more slowly adhered, which demonstrates that the wettability of the surface is insignificant at higher speed.[23] From movies taken with the high-speed camera, we measured the speed of the droplet U based on the displacement of the center of the droplet divided by the time interval between two consecutive images; the size of the droplets D was characterized as the length of the droplets. In the experiments, we first drive the droplets to move at a speed high enough for the droplets to pass through the hydrophobic section, and then we gradually reduced the flow velocity in order to determine the critical speed to induce adhesion. Next, we varied the size of the droplets and found that the critical velocity for adhesion increased as the droplet size increased.

The influence of drop size and flow speed on adhesion can be summarized in a phase diagram as shown in Figure 3(a),

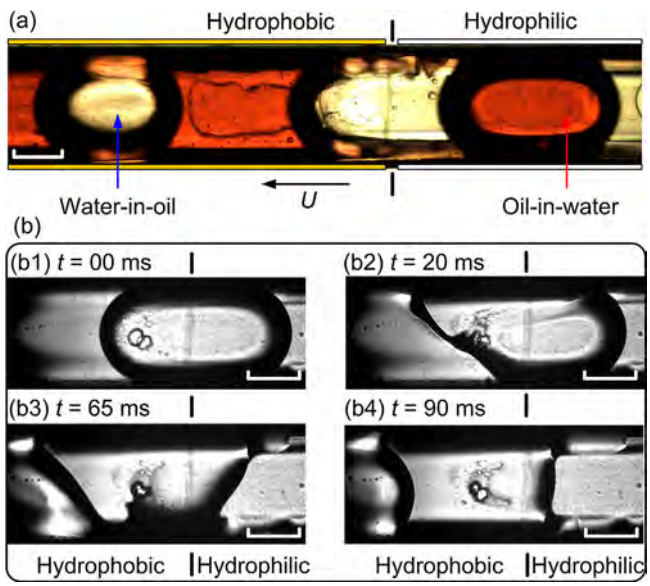

FIG. 2. Observation of droplet adhesion inside a capillary with modified wettability. To the right of the vertical black line, the capillary was untreated while the inner surface to the left of the line was coated with OTS. (a) Oil-in-water droplets flow from the hydrophilic section into the hydrophobic section of the capillary. The oil phase was dyed red. (b) Images documenting the rapid adhesion process of an oil droplet. The droplet is moving from right to left. Adhesion was observed to start at the front part of the droplet. The translation speed of the droplet in (a) is 2.43 mm/s and in (b) is 2.62 mm/s. Scale bars are 500 μm and the inner dimension of the capillary is 1.05 mm (enhanced online) [URL: http://dx.doi.org/10.1063/1.4823456.1] [URL: http://dx.doi.org/10.1063/1.4823456.2].

where the axes are the dimensionless capillary number $Ca = \mu U/\gamma$ and the dimensionless ratio of the length of the droplet to the inner dimension of the square capillary, D/d. When plotted with logarithmic axes, the experimental results of the critical capillary number fall roughly onto straight lines where each line corresponds to a different size square capillary. The results indicate that for droplets with the same size, adhesion can be induced by lowering the translation speed, while for droplets moving with a constant speed, adhesion can be generated by increasing the droplet size. Also, the critical capillary number was found to decrease as the capillary size increased, which indicated that droplet adhesion induced by the change of the capillary surface wettability happened more easily in smaller capillaries at relatively higher translation speeds of the droplets.

Adhesion will occur when the oil-water interface enters the interaction range of the attractive van der Waals force. However, in the experiments, the interface still needs to overcome the thin lubrication film formed between the moving oil droplet and the microchannel wall. Therefore, for adhesion, the lubrication film needs to be thin enough that the van der Waals force is equal to or larger than the Laplace pressure on the droplet interface in order to pull it onto the wall, as sketched in Figure 3(b). In these experiments, the thickness of the lubrication film h_0 is related to the capillary number according to $h_0/d \sim Ca^{2/3}$, as first analyzed by Bretherton,[22] and so higher speeds correspond to thicker more stable films. Although the Bretherton result was derived for bubbles, a similar scaling holds for drops.[24]

In this experiment, when the droplet was moving in the untreated section of the glass capillary, the thickness of the lubrication film was much larger than the interaction range of the van der Waals force, and no adhesion occurred. But when the droplet was moving into the hydrophobic section of the capillary, the additional long range hydrophobic force acted on the oil-water interface. The altered force caused the instability of the interface, which made the oil-water interface much closer to the capillary surface, and the van der Waals force on the oil-water interface was increased. When the van der Waals force was equal to the Laplace pressure, the adhesion started. The strength of the van der Waals force is given by the film thickness (h) dependent disjoining pressure $\Pi(h) = A/(6\pi h^3)$, where A is the Hamaker constant. Since A lies in the range $(0.4\text{–}4) \times 10^{-19}$ J for most condensed phases,[16] here we use the typical value of $A = 1 \times 10^{-19}$ J in the calculations below. The corresponding Laplace pressure at a curved nearly cylindrical interface is $p_s = \gamma/r_c$, where r_c is the radius of the curvature, which for a sinusoidally varying interface of wavelength λ and amplitude a is approximately $r_c \sim \lambda^2/a$. For adhesion to occur, the wave amplitude a is approximately h_0, and we expect λ approximately D, the size of the droplet. Therefore, according to the force balance equation $\Pi(h) = p_s$, we obtain

$$(A/\gamma)D^2 \sim {h_0}^4. \tag{1}$$

Combining the Bretherton equation $h_0/d \sim Ca^{2/3}$ and Eq. (1), we obtain a relation between the critical capillary number for adhesion and the droplet size in the form

$$Ca = k\left(\frac{A}{\gamma d^2}\right)^{3/8}\left(\frac{D}{d}\right)^{3/4}, \tag{2}$$

where k is a constant. Figure 3(c) plots the relationship between $Ca \times d^{3/4}$ and D/d for the three different size capillaries. The normalized experiment results collapse and are almost in superposition, and the slope of $Ca \times d^{3/4}$ versus D/d in the log-log plot is close to the theoretical predicted value of 3/4. Therefore, our order-of-magnitude model is able to rationalize the experimental results as U, d, and D are varied. Moreover, the constant $k = 2.5$ is obtained by the fitted line of the experimental results in Figure 3(c).

The control of adhesion during droplet motion can be used to realize a separation process, targeted release, and other applications in lab-on-a-chip systems. Here, we demonstrate how to use droplet adhesion to recycle the ingredient materials of emulsions in microfluidics. For example, emulsion droplets are used in many lab-on-a-chip applications, such as encapsulation, delivery, and separation. In some applications, the materials of the emulsions are valuable and so recycling is needed. However, typically the emulsions are stable and not easily broken down to two separated phases. As a specific example, for a typical oil-in-water emulsion system, where silicone oil (Dow Corning 200® Fluid, 20 cst)

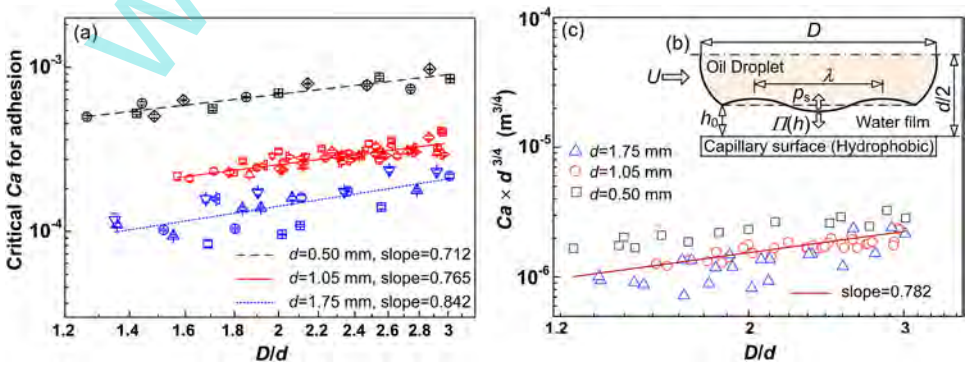

FIG. 3. Critical capillary number for adhesion. (a) Phase diagram of droplet adhesion as a function of the critical capillary number $Ca = \mu U/\gamma$ and the ratio of the droplet length D to the capillary size d. The different symbols indicate the experiments performed in several different capillaries with the inner dimension of 0.5 mm, 1.05 mm and 1.75 mm, respectively, and the three lines are the corresponding best fits of the measured critical capillary number for each size of capillary. (b) Schematic of the droplet moving from the hydrophilic part to the hydrophobic part of the capillary, where the altered surface force causes the disruption of the oil-water interface. (c) The relationship of the normalized experimental results of $Ca \times d^{3/4}$ versus D/d. The symbols are the normalized experimental results, while the continuous line is the best fit of all the experimental results. The value of the slope is obtained from the fitted line.

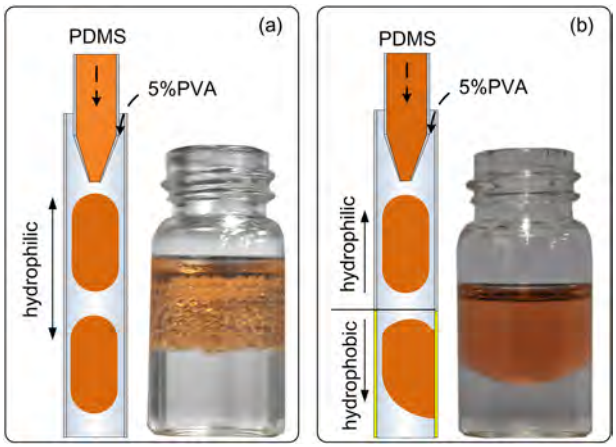

FIG. 4. Application of the droplet adhesion technology for the recycling of emulsion droplets. The oil emulsions were dyed red. (a) Oil emulsions were translating in the untreated capillary, and they retained the emulsion structure after collection. (b) Adhesion of the emulsion droplets occurred in the hydrophobic part of the capillary, the emulsion droplets broke up, and the oil phase was separated from the water phase after collection.

is the droplet phase and an aqueous solution of 5 wt. % PVA is the continuous water phase, where PVA is playing the role of a surfactant, the collected emulsion droplets still remain a stable emulsion and the oil droplets are mixed with the water phase, as shown in Figure 4(a). However, when we use the technology of droplet adhesion illustrated above, then below a critical speed the oil emulsion droplets formed in the hydrophilic region will break up in the hydrophobic region. Thus, we can separate the oil phase from the water phase and collect the pure oil phase from the original emulsion fluids, as shown in Figure 4(b).

During flow in microfluidic devices, emulsion droplets are isolated from the channel wall by a thin lubricating film of the continuous phase and higher droplet speeds correspond to thicker films. However, we found that the change of the surface wettability may cause the instability of this lubricating film below a critical drop speed, where the film thickness is smaller, and subsequently, there is adhesion of emulsion droplets to the walls of the channel. For a drop of size D (greater than the capillary dimensions d), the critical capillary number for droplet adhesion is approximately $Ca \sim D^{3/4}/d^{3/2}$, which can be rationalized when the lubrication film becomes thin enough for the van der Waals force to balance the Laplace pressure of the perturbed droplet interface. Finally, we demonstrated that the adhesion of translating droplets can offer a route for the recycling of emulsions in many applications of microfluidics.

This work was supported by the NSFC (Nos. 51275266 and 51275036). The authors thank Isabelle Cantat, Camille Duprat, Jens Eggers, Naima Hammoud, and Peichun Amy Tsai for helpful discussions, and we also thank Bing Dong for support of the experiments.

[1]P. Roach, N. J. Shirtcliffe, and M. I. Newton, Soft Matter **4**, 224 (2008).
[2]K. Koch, B. Bhushan, and W. Barthlott, Prog. Mater. Sci. **54**, 137 (2009).
[3]H. Y. Erbil, A. L. Demirel, Y. Avci, and O. Mert, Science **299**, 1377 (2003).
[4]B. Bhushan, Y. C. Jung, and K. Koch, Langmuir **25**, 3240 (2009).
[5]D, Quere, Annu. Rev. Mater. Res. **38**, 71 (2008).
[6]H. A. Stone, A. D. Stroock, and A. Ajdari, Annu. Rev. Fluid Mech. **36**, 381 (2004).
[7]R. K. Shah, H. C. Shum, A. C. Rowat, D. Lee, J. J. Agresti, A. S. Utada, L. Y. Chu, J. W. Kim, A. Fernandez-Nieves, C. J. Martinez, and D. A. Weitz, Mater. Today **11**, 18 (2008).
[8]A. S. Utada, E. Lorenceau, D. R. Link, P. D. Kaplan, H. A. Stone, and D. A. Weitz, Science **308**, 537 (2005).
[9]J. Wan, A. Bick, M. Sullivan, and H. A. Stone, Adv. Mater. **20**, 3314 (2008).
[10]S. L. Anna, N. Bontoux, and H. A. Stone, Appl. Phys. Lett. **82**, 364 (2003).
[11]E. Brouzes, M. Medkova, N. Savenelli, D. Marran, M. Twardowski, J. B. Hutchison, J. M. Rothberg, D. R. Link, N. Perrimon, and M. L. Samuels, Proc. Natl. Acad. Sci. U.S.A. **106**, 14195 (2009).
[12]J. J. Agresti, E. Antipov, A. R. Abate, K. Ahn, A. C. Rowat, J. C. Baret, M. Marquez, A. M. Klibanov, A. D. Griffiths, and D. A. Weitz, Proc. Natl. Acad. Sci. U.S.A. **107**, 4004 (2010).
[13]H. Zhang, E. Tumarkin, R. Peerani, Z. Nie, R. A. Sullan, G. C. Walker, and E. Kumacheva, J. Am. Chem. Soc. **128**, 12205 (2006).
[14]S. Wang, K. Liu, and J. Liu, Angew. Chem., Int. Ed. **50**, 3084 (2011).
[15]E. G. Jehad, K. Benson, and L. De Cola, Angew. Chem., Int. Ed. **51**, 3716 (2012).
[16]J. Israelachvili, *Intermolecular & Surface Forces* (Academic, London, 1994).
[17]H.-J. Butt, B. Cappella, and M. Kappl, Surf. Sci. Rep. **59**, 1 (2005).
[18]W. A. Ducker, T. J. Senden, and R. M. Pashley, Nature **353**, 239 (1991).
[19]R. R. Dagastine, R. Manica1, S. L. Carnie1, D. Y. C. Chan, G. W. Stevens, and F. Grieser, Science **313**, 210 (2006).
[20]I. U. Vakarelski, R. Manica, X. Tang, S. J. O'Shea, G. W. Stevens, F. Grieser, R. R. Dagastine, and D. Y. C. Chan, Proc. Natl. Acad. Sci. U.S.A. **107**, 11177 (2010).
[21]E. Klaseboer, J. P. Chevaillier, C. Gourdon, and O. Masbernat, J. Colloid Interface Sci. **229**, 274 (2000).
[22]F. P. Bretherton, J. Fluid Mech. **10**, 166 (1961).
[23]G. F. Teletzke, H. T. Davis, and L. E. Scriven, Rev. Phys. Appl. **23**, 989 (1988).
[24]S. R. Hodges, O. E. Jensen, and J. M. Rallison, J. Fluid Mech. **501**, 279 (2004).
[25]G. Paradossi, F. Cavalieri, and E. Chiessi, J. Mater. Sci.: Mater. Med. **14**, 687 (2003).